A LETTERS JOURNAL EXPLORING THE FRONTIERS OF PHYSICS

Laser absorption in microdroplet plasmas

To cite this article: M. Anand *et al* 2007 *EPL* **80** 25002

A LETTERS JOURNAL EXPLORING THE FRONTIERS OF PHYSICS
October 2007
EPL, **80** (2007) 25002 www.epljournal.org
doi: 10.1209/0295-5075/80/25002

Laser absorption in microdroplet plasmas

M. ANAND[1], P. GIBBON[2] and M. KRISHNAMURTHY[1]

[1] *Tata Institute of Fundamental Research - 1 Homi Bhabha Road, Mumbai 400 005, India*
[2] *John-von-Neumann Institute for Computing, ZAM, Forschungszentrum Jülich - D-52425 Jülich, Germany*

received 19 June 2007; accepted in final form 24 August 2007
published online 14 September 2007

PACS 52.38.Ph – X-ray, γ-ray, and particle generation
PACS 52.25.Os – Emission, absorption, and scattering of electromagnetic radiation
PACS 79.20.Ds – Laser-beam impact phenomena

Abstract – We present experimental measurements of the absorption of ultrashort laser pulses by 15 μm diameter methanol microdroplets. The droplet absorbs upto 70% of the incidence laser energy in the presence of a prepulse at intensities of about $1.5 \times 10^{16}\,\mathrm{W\,cm^{-2}}$. In the absence of a prepulse, the absorption is only about 20%. Simultaneous measurements of X-ray yield (12 keV to 350 keV) and the absorption in the droplet plasma, shows that our earlier measurements of efficient generation (ANAND M. *et al. Appl. Phys. Lett.*, **88** (2006) 181111) of hard X-rays from the droplet plasma is due to the increased absorption in the droplets in the presence of optimum prepulse. 1-D PIC simulations, mimicing the mass-limited droplet density profile, demonstrate the effectiveness of the large scale-length droplet plasma in providing optimal conditions for resonant laser absorption energy and generation of hot electrons.

Intense laser interaction with matter is of interest not only because of the non-linear interaction physics prevalent at extreme temperatures and densities, but also due to the numerous applications which have arisen. Laser-produced plasmas are promising sources for applications in, for example, lithography [1], X-ray diffraction studies [2], electron and ion acceleration [3]. The novelty in probing different dynamics arises not only through the intensity but also from the form of matter used to create the plasma. Depending on the characteristics of the matter that absorbs the laser energy, namely its size, density and scale length, the interaction dynamics and the efficiency of absorption, X-ray production may be controlled. One form of matter that has been recently studied is tiny microdroplets of 10–20 μm diameter. These droplets offer the advantage of high density similar to that of solids, but are mass-limited. They have been found to be advantageous in applications such as EUV lithography [1] compared to other targets, owing to both efficiency of EUV production and for being largely free from debris. The spherical geometry of the size-limited target brings out new features in the interaction physics that are not normally accessed with conventional solid slab targets [4,5]. For intensities up to $10^{13}\,\mathrm{W\,cm^{-2}}$, it has been shown experimentally that (for the droplets that are about 10 times larger than the incident light wavelength) the incident light is Mie scattered into the drop resulting in nanospots in the drop where the intensities are 100 times larger [6]. Plasma is efficiently formed in these hot nanospots that are spatially spread out in and around the droplet, essentially creating an efficient preplasma sphere. An intense main pulse incident on such a plasma ball of optimum density would interact very differently compared to a plain slab targets. Our earlier experiments have shown that the hard X-ray generation (50–150 keV) can be as large 68 times that observed from the plain slab targets at an intensity of $2 \times 10^{15}\,\mathrm{W\,cm^{-2}}$. These manifestations are attributed to qualitative differences due to geometric effects, which influence the way the incident laser energy is coupled into the matter.

The production of charged particles or X-rays from laser-produced plasmas depends on the amount of laser radiation absorbed by the system. It has been found that solid targets absorb incident laser energy anywhere between 15 and 70% at intensities of about $10^{16}\,\mathrm{W\,cm^{-2}}$ [7]. In gaseous van der Waals clusters, laser absorption as large as 90% had been demonstrated [8]. With both types of target the amount of laser energy absorbed strongly depends on the pulse characteristics, namely intensity, pulse width, polarization etc., essentially because the absorption mechanism varies depending on the incident intensity. One should also keep in mind that in plain slab targets the absorption mechanism differs with the angle of incidence and also whether the light is S polarized or P polarized. In clusters, on the other hand, where the size of the target is much smaller than the wavelength, other issues related to size and geometric effects play a role. In all the systems, clusters and solids, the measurement of the absorbed energy is an important parameter that can be used to identify the dynamics of the interaction. Correlations between the absorbed laser energy and hot electron production have been made previously for solid-density plasmas [9]. Experimental measurements of femtosecond laser absorption by few-micron–sized droplets are to date still limited [10]. Recently, absorption measurements were made on sub-micron droplets with 2 ps laser pulses, in which higher absorption was observed with the droplets [11]. Wu *et al* [12] have estimated the amount of energy absorbed by liquid droplets using resonance absorption for short scale lengths and compare the hot electron angular distribution from the droplet. They calculate a maximum absorption of about 20% at a density scale length of $L/\lambda = 0.17$ for droplets of 5 μm diameter.

In the present paper, we demonstrate the influence on the prepulse in enhancing the absorption of the laser energy in 15 μm droplets. Before we describe the results of the absorption, we briefly report on our recent measurements with the 15 μm methanol droplet under irradiation with intense pulses up to 2×10^{16} W cm^{-2}. The droplets in this regime produce hot electrons which result in bremsstrahlung radiation up to 350 keV in the presence of a prepulse [5]. We have made a direct comparison of the hard X-ray emission (50–150 keV) from the droplet target with a plain slab target under similar laser irradiation and prepulse. The threshold for the hard X-ray generation is much lower with the droplet target and the X-ray emission is about 68 times larger compared to the solid target of similar composition at an intensity of 2×10^{15} W cm^{-2} [4]. The hot electron temperature with the droplets is as large as 36 keV even at intensities as small as 2×10^{15} W cm^{-2}. In the present paper, we discuss the simultaneous measurement of the hard X-rays and the absorption in order to correlate that the enhanced efficiency of X-ray emission from the droplet is due to an increase in absorption of the laser energy in the presence of the prepulse.

A detailed description of the apparatus made to deliver the droplets in vacuum for the purpose of intense laser studies can be found in [5]; only a brief description of important features for the absorption measurements are given here. The microdroplet target is generated by forcing methanol through a 10 μm capillary vibrating at a frequency of about 1 MHz. The liquid jet breaks spontaneously into uniformly sized microdroplets. Measurements on the characterization of the droplet jet revealed the production of a very uniformly sized stream of methanol droplets of 15 μm in diameter [13]. We had earlier measured, through elaborate morphological dependent resonances (MDR) in the fluorescence emission from the dye doped drops, that the fluctuation in the size of the drop is at most 10% [5]. The droplet stream is injected into a vacuum chamber that is maintained at 10^{-2} torr with the droplet load by differential pumping. The overlap between the laser focal spot and the droplets was monitored continuously using a CCD camera.

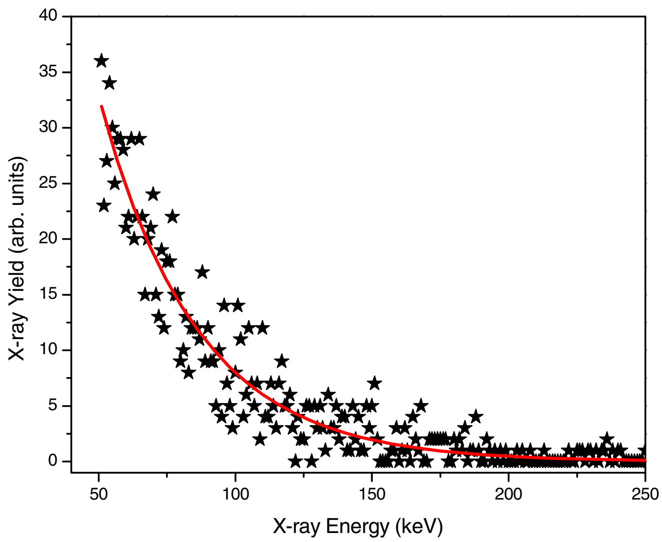

Fig. 1: Typical X-ray spectrum measured with the 15 μm droplet in the intensity regime of 10^{14} to 10^{16} W cm^{-2}. The solid line shows a Maxwellian fit to the data, demonstrating an electron temperature of 35 keV observed at an intensity of 2×10^{15} W cm^{-2}.

The experiment was carried out using a 7 TW, Ti:sapphire laser system, producing 60 fs laser pulses at a wavelength of 800 nm. For present experiments we only use laser pulses of about 10 mJ in energy/pulse. The incident light is focused to a maximum intensity of about 2×10^{16} W cm^{-2} using a 30 cm focal length f/7 lens. The focal spot size is measured to be 30 μm, which is about twice the size of the droplet. In prepulse experiments, the incident beam was split into two parts using a combination of a thin film polarizer and a $\lambda/2$ plate and the main pulse was delayed by about 10 ns using an optical delay line. The energy of the first pulse (prepulse) is independently varied with respect to the main pulse of higher intensity.

The hard X-ray measurements were made using a NaI scintillator detector coupled to pulse-counting electronics and computerized data acquisition. The detector is calibrated with standard radioactive sources and gated with the laser pulse to avoid background. A detailed description of the X-ray measurements from the droplets under different laser conditions, polarization, intensity, etc., is published in our earlier work [4,5,14] and here we give only some of the essential features of hard X-ray generation. Figure 1 shows the X-ray spectrum, measured at an intensity of 2×10^{15} W cm^{-2} in the range of 50–250 keV with the NaI detector. We use the calibrated pulse height measurements of the scintillation to determine the X-ray energy. The detector is placed in air at about 60 cm from the droplet and the solid angle of the data collected is reduced by using a 5 mm aperture in

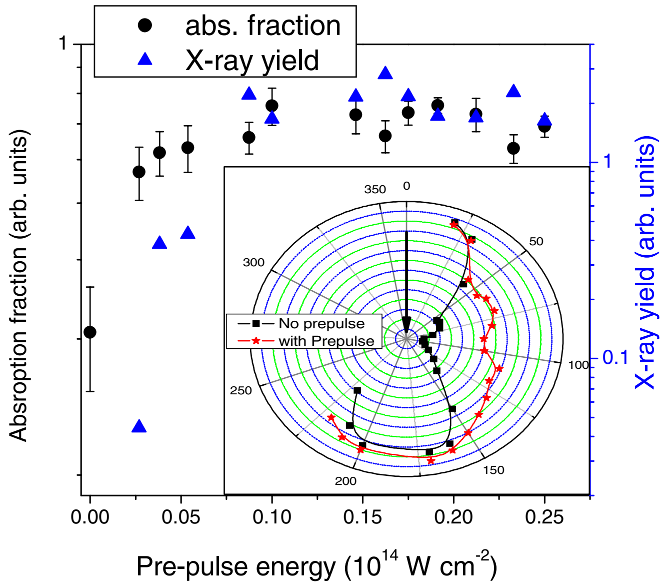

Fig. 2: The absorption of the incident laser energy at various prepulse fractions measured as attenuation of the pulse energy in transmission through the droplet. The main pulse intensity is $1.3 \times 10^{16}\,\mathrm{W\,cm^{-2}}$. The hard X-ray yield at the corresponding prepulse fraction is also shown. The inset shows the angular distribution of the scattered light measured both in the presence and absence of a prepulse. Lines are drawn to guide the eye. The arrow indicates the laser propagation direction.

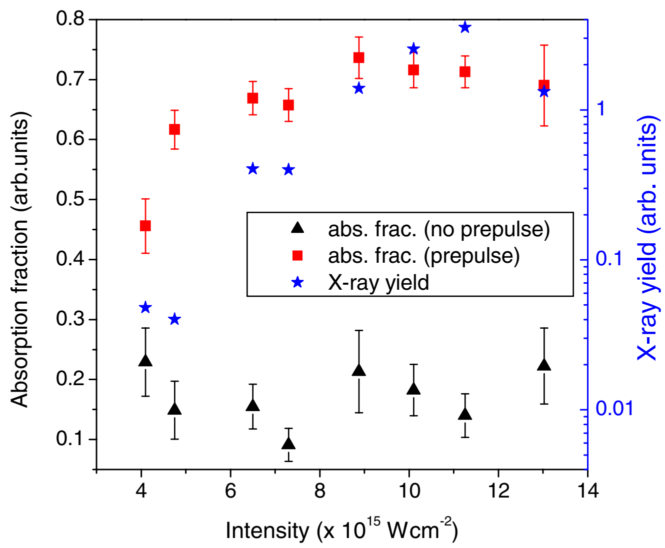

Fig. 3: The attenuation in the presence and the absence of a prepulse at various incident laser intensities. Also shown is the X-ray yield in the presence of a prepulse at the corresponding intensity.

the 1 cm thick lead enclosure that surrounds the detector. To ensure that there is no pile up at the detector and the spectral measurements are accurate, the count rate is reduced to 0.1 count/laser shot. We fit the measured spectrum with a Maxwellian distribution, as shown with the solid curve in fig. 1 and we infer the hot electron temperature to be about 35 keV.

The absorption was calculated by measuring the transmitted, the scattered energy and the back reflection. The transmitted laser energy was measured using a power meter. The scattered light was measured using well calibrated photodiodes that are scanned over an angle of 180 degrees. Shot-to-shot fluctuation in the input energy was also measured using a photodiode. The scattering losses integrated over 4π solid angle was measured to be about 1% at intensities of about $2 \times 10^{16}\,\mathrm{W\,cm^{-2}}$ in the absence of a prepulse and only marginally higher, about 1.5% in the presence of the prepulse. There is no measurable backscattered signal above 4% background reflection that is expected from the uncoated glass window of the vacuum chamber and the lens, the measured signal is unaffected by the presence of the droplet at the focus or absence of it. The transmission was measured as an average over 200 shots with the power meter.

Before we discuss the absorption measurements, we first present the scattered laser energy from the droplet preplasma as shown in inset of fig. 2. The scattering is predominantly along the laser propagation direction, much like the scatter expected by the Mie scattering from particles that are few times larger than the incident light wave length. The total scattered energy in the presence of a prepulse is less than 1.5% of the incident laser energy. The scattered light intensity along the beam propagation direction does not change much in the presence or the absence of the prepulse. As expected, the scattering is enhanced in the presence of the prepulse at 90° to the laser direction. The droplet is expanded to about $30\,\mu$m diameter due to the prepulse [5]. The expansion of the mass-limited target leads to a lowered density, allowing increased refraction from the resulting spherical plasma ball and thus more scattering in the perpendicular direction.

We first establish the importance of a prepulse in the absorption of the incident laser energy in a micro-droplet plasma. The absorption of the incident laser energy with increase in the fraction of an identical prepulse that arrives 10 ns ahead of the main pulse is shown in fig. 2. The main pulse intensity in these measurements is $1.3 \times 10^{16}\,\mathrm{W\,cm^{-2}}$. The absorption changes dramatically from about 20% to about 60% when there is a prepulse. A prepulse fraction of 5% causes the absorption to saturate at about 60–70%. Also shown in the plot is the hard X-ray yield for various prepulse fractions. The simultaneous measurement of the absorption clearly shows that a prepulse of about 2% is essential for hard X-ray from microdroplet [5] at these intensities. The plot clearly indicates that both the X-ray and the absorption saturate beyond a certain fraction of the prepulse energy.

We also measured absorption as a function of intensity of the main pulse for a given prepulse energy. Figure 3 shows the measured attenuation both in the presence and the absence of the prepulse. In the absence of a prepulse the maximum absorption is about 20% whereas with a

10% prepulse the maximum absorption is about 70%. The error bars in the absorption measurement are essentially because of the intensity fluctuation due to the droplet jitter in the focal volume. The figure clearly shows that the absorption fraction increases from about 45% to about 70% with intensity in the presence of the prepulse. On the other hand, the absorption does not vary much in the absence of prepulse. The absorption fraction of about 20% in the absence of prepulse in the case of a droplet plasma at our intensities agrees well with other absorption measurement shown for dielectric solid targets [15]. It should be noted that in the absence of the prepulse, the droplet is smaller than the focal waist of the incident laser beam and that the droplet is exposed to only 38% of the incident laser power. This indicates that droplet might be similar to solid dielectric targets as far as absorption is concerned in the absence of a prepulse. Droplet targets have been shown to produce negligible hard X-rays in the absence of a prepulse [4], especially, for the droplet sizes used in these experiments and for intensities up to $2 \times 10^{16}\,\mathrm{W\,cm^{-2}}$.

Also shown in fig. 3 is the hard X-ray yield from microdroplet plasma in the presence of a prepulse. Increase in absorption brings about an increase in the X-ray emission. The X-ray yield, however, shows a sharper rise with intensity compared to the absorption fraction indicating that the higher hot electron fraction at larger intensity is more due to the higher conversion fraction of the absorbed energy into hot electrons than on the higher absorption fraction directly. At intensities above $5 \times 10^{15}\,\mathrm{W\,cm^{-2}}$, the change in the absorption of about 10% produces about 90 times enhanced X-ray yield.

We have shown in our earlier work [5] that the geometric effects of the size limited target are very important. A prepulse of intensity less than $10^{14}\,\mathrm{W\,cm^{-2}}$, would undergo Mie scattering inside the drop and effectively focus the incident electro magnetic radiation inside the drop [6]. Our calculations reveal that for our droplet size, and the 800 nm light pulses, the intensity enhancement at the nanometer hot spots inside the drop can be 100 fold. The hot spots in and about the drop are effective in producing a spherical plasma ball. The higher the prepulse energy, the higher is the efficiency of the preplasma formation and the expansion of the plasma ball expands, before the main pulse arrives. In the presence of a prepulse, the droplet expands to nearly twice its initial size after 10 ns. The main pulse thus samples a large volume, large scale length preplasma, that is very effective at absorbing the incident laser energy and converting it into hard X-ray emission.

These geometric effects can be completely modeled only by 3D PIC (particle in cell) simulations. Nevertheless we can still gain insight into the effect of large scale length preplasma by sampling the plasma along a radial line in one dimension. To this end, we have performed high-resolution 1D PIC simulations with different density profiles that qualitatively mimic those from the droplet.

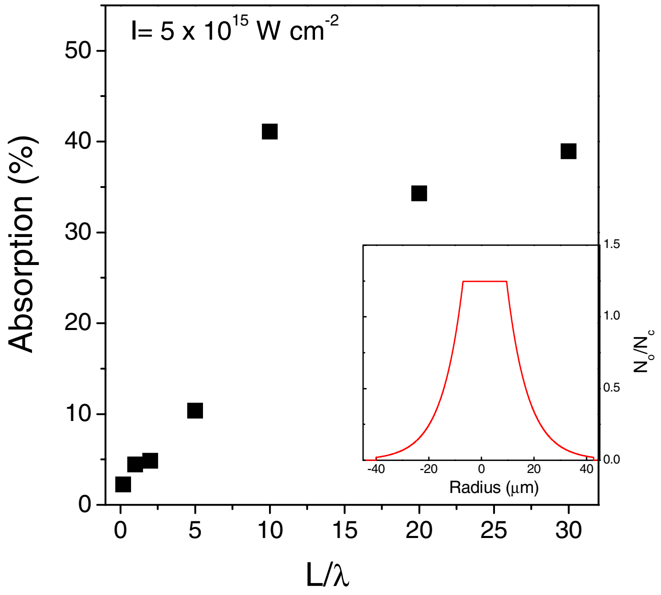

Fig. 4: Computed absorption fraction of the incident laser energy for different scale lengths. 1D PIC simulations with a mass limited droplet profile (shown in the inset) is used at incident light intensity of $5 \times 10^{15}\,\mathrm{W\,cm^{-2}}$. N_0 is the electron density and N_c is the critical electron density at the incident light wave length.

Figure 4 shows the results of the simulations performed using BOPS, a 1D2V PIC code, which exploits the Lorentz boost technique to handle oblique-incidence interactions [16,17]. The angle of incidence in the computations is kept at 15°. In our earlier studies we have correlated the hot electron energy distributions with the experimental measurements. A series of calculations with different scale length showed a fivefold increase in electrons above 20 keV and an onset of super hot electrons (50 keV) as the profile is stretched from an abrupt step to an extended corona. In the present paper we only present the calculated absorption.

In fig. 4 we show the total absorption of the incident radiation for various initial density scale lengths, keeping the total target mass (or charge) conserved. As the prepulse fraction is increased, the droplet expands and the scale length of the plasma sampled by the main pulse is increased. Figure 2 shows that as the prepulse intensity is increased or if the scale length of the plasma is made larger, the absorption of the incident laser light is larger. The results from the numerical simulation support this observation, as seen in fig. 4, the absorption fraction increases with the scale length and saturates at about a L/λ of 10, much like the measurements shown in fig. 2. From our earlier measurements of the expansion of the droplet due to the prepulse [5] and estimates made for the plasma scale length from an isothermal model [4], we expect density profiles with $L/\lambda > 10$ for the droplet preplasma. The larger density scale length of the droplet plasma favors the absorption of the laser light via resonance absorption and the associated hot electron production. Our earlier computations of the hot electron yield as a function of the scale length in a size limited target were also consistent with this experimentally observed feature [4]. We should stress that these computational results only permit a qualitative comparison, and indicate a trend of higher absorption with increasing scale length, saturating at larger scale lengths.

To summarize, we have measured absorption up to 70% from 15 μm diameter methanol microdroplets in the presence of a prepulse that arrived 10 ns before the main laser pulse. The absorption in the absence of a prepulse is only about 20%. The hot electron production is correlated with the absorption measurements for lower intensities and in the presence of a prepulse. At higher intensities, the hot electron production is more efficient indicating a better efficiency of conversion of the absorbed energy into X-rays. 1D PIC simulations with the mass limited droplet density profile show that the increase in the scale-length of the plasma brings about enhanced absorption of the laser energy as the main pulse interacts with the large volume and optimum density preplasma.

REFERENCES

[1] Malmqvist L., Rymell L. and Hertz H. M., *Appl. Phys. Lett.*, **68** (1996) 2627.

[2] Rischel C., Rousse A., Uschmann I., Albouy P. A., Geindre J. P., Audebert P., Gauthier J. C., Forster E., Martin J. L. and Antonetti A., *Nature (London)*, **390** (1997) 490.

[3] Fuchs J., Antici P., d'Humières E., Lefebvre E., Borghesi M., Brambrink E., Cecchetti C. A., Kaluza M., Malka V., Manclossi M., Meyroneinc S., Mora P., Schreiber J., Toncian T., Pépin H. and Audebert P., *Nat. Phys. (London)*, **2** (2006) 48.

[4] Anand M., Sandhu A. S., Kahaly S., Ravindra Kumar G., Krishnamurthy M. and Gibbon P., *Appl. Phys. Lett.*, **88** (2006) 181111.

[5] Anand M., Safvan C. P. and Krishnamurthy M., *Appl. Phys. B*, **81** (2005) 469.

[6] Favre C., Boutou V., Hill S.C., Zimmer W., Krenz M., Lambrecht H., Yu J., Chang R. K., Woeste L. and Wolf J. P., *Phys. Rev. Lett.*, **89** (2002) 35002.

[7] Gibbon P., *Short Pulse Laser Interactions with Matter* (Imperial College Press, London) 2005.

[8] Ditmire T., Smith R. A., Tisch J. W. G. and Hutchinson M. H. R., *Phys. Rev. Lett.*, **78** (1997) 3121.

[9] Teubner U., Uschmann I., Gibbon P., Altenbernd D., Förster E., Feurer T., Theobald W., Sauerbrey R., Hirst G., Key M. H., Lister J. and Neely D., *Phys. Rev. E*, **54** (1996) 4167.

[10] Peng X. Y., Zhang J., Jin Z., Liang T. J. and Sheng Z. M. *et al.*, *Phys. Rev. E*, **69** (2004) 026414.

[11] Gumbrell E. T., Comley A. J., Hutchinson M. H. R. and Smith R. A., *Phys. Plasmas*, **8** (2001) 1329.

[12] Wu H. C., Yu W., Liang T. J., Peng X. Y., Jin Z., Li Y. J., Sheng Z. M., Tang X. W. and Zhang J., *Appl. Phys. B*, **77** (2003) 687.

[13] Anand M., Dharmadhikari A. K., Dharmadhikari J. A., Mishra A., Mathur D. and Krishnamurthy M., *Chem. Phys. Lett.*, **372** (2003) 263.

[14] Anand M., Gibbon P. and Krishnamurthy M., *Laser Phys.*, **17** (2007) 408.

[15] Price D. F., More R. M., Walling R. S., Guethlein G., Shepherd R. L., Stewart R. E. and White W. E., *Phys. Rev. Lett.*, **75** (1995) 252.

[16] Gibbon P. and Bell A. R., *Phys. Rev. Lett.*, **68** (1992) 1535.

[17] Gibbon P., Andreev A. A., Lefebvre E., Bonnaud G., Ruhl H., Delettrez J. and Bell A., *Phys. Plasmas*, **6** (1999) 947. The BOPS code is available online at `http://www.fz-juelich.de/zam/cams/plasma/BOPS/`.